Magnetic Structure of $ErFeO_3$ below 4.5 °K

G. Gorodetsky*
Department of Physics, University of the Negev, Beer-Sheva
Department of Electronics, The Weizmann Institute of Science, Rehovot, Israel

R. M. Hornreich* and I. Yaeger*
Department of Electronics, The Weizmann Institute of Science, Rehovot, Israel

H. Pinto, G. Shachar, and H. Shaked
Department of Physics, Nuclear Research Center-Negev, Beer-Sheva, P.O.B. 9001, Israel

(Received 6 April 1973)

Using long-wavelength ($\lambda \sim 2.4$ Å) neutrons, diffraction patterns of $ErFeO_3$ were taken at 140, 4.2, and 1.5 °K. Two possible structures for the Fe^{3+} spin system at 1.5 °K were found to be consistent with the neutron data. Both of the possible structures belong to the antiferromagnetic G configuration. In the first, the Fe^{3+} antiferromagnetic axis is in the orthorhombic ab crystallographic plane at an angle of $33° \pm 4°$ to the b axis. In the second, the Fe^{3+} antiferromagnetic axis is in the bc plane at an angle of $51° \pm 8°$ to the b axis. Magnetization and torque measurements showed that the spontaneous moment is along the a axis for all temperatures below that of liquid nitrogen. It exhibits a sharp peak at $T \sim 4.5$ °K, thereafter dropping sharply with decreasing temperature. This result is consistent only with the latter of the two possible structures. Thus, for $T < 4.5$ °K, the Fe^{3+} spins are in essentially a mixed G_{yz} mode rather than the G_{xy} mode suggested previously. It is concluded that a reorientation of the Fe^{3+} antiferromagnetic axis from the c axis (at 4.5 °K) toward the b axis takes place as the temperature is decreased below 4.5 °K. Possible mechanisms responsible for this low-temperature spin reorientation are reviewed.

I. INTRODUCTION

The rare-earth orthoferrites, $RFeO_3$, crystallize in an orthorhombically distorted perovskite structure.[1] This structure belongs to the space group D_{2h}^{16}–$Pbnm$ with R in the (4c) and Fe in the (4b) positions as shown in Fig. 1. The possible magnetic configurations with symmetry isomorphic[2] to D_{2h}^{16} were defined by Wollan and Koehler[3] and by Bertaut[4] and are listed in Table I. The possible magnetic structures with symmetry isomorphic[5] to D_{2h}^{16} have also been classified by Bertaut according to their magnetic symmetry, and this classification is given in Table II.

Immediately below the ordering temperature the Fe^{3+} magnetic structure in the rare-earth (RE) orthoferrites is that of a "canted antiferromagnet." More specifically, they exhibit an essentially antiferromagnetic structure G_x (i.e., a $\vec{G}$ configuration with its spin axis parallel to the a crystallographic axis) with an accompanying weak ferromagnetic structure F_z.[6–8] As seen in Table II, G_x and F_z belong to the magnetic space group $Pb'n'm$. This means that the product F_zG_x is invariant under the operations of the symmetry elements of the paramagnetic space group $1'Pbnm$.

As the temperature is lowered, the Fe^{3+} spins in some of the RE orthoferrites exhibit a spin reorientation. That is, they undergo a transition to a different magnetic structure, which is usually the canted antiferromagnetic structure G_zF_x.[6,7] G_z and F_x belong to $Pbn'm'$ and the product G_zF_x is therefore also $1'Pbnm$ invariant.

Turning to the case of $ErFeO_3$, the weak ferromagnetism of this compound was studied by Bozorth *et al.*[6] and its antiferromagnetic structure was first investigated by Koehler *et al.*[9] These and later

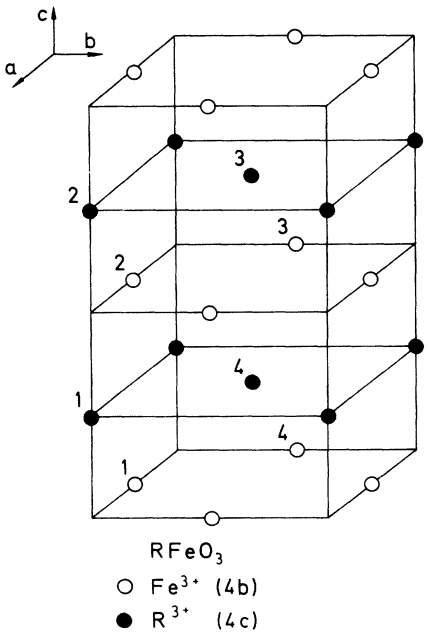

FIG. 1. Orthorhombic unit cell of $RFeO_3$. Only the R^{3+} and Fe^{3+} ions are shown.

TABLE I. Definition of magnetic configurations (Refs. 3 and 4).

Configuration designation	site 1	2	3	4
F	+	+	+	+
G	+	−	+	−
A	+	−	−	+
C	+	+	−	−

studies by other workers[7,8] led to the conclusions on the magnetic structure of $ErFeO_3$ summarized in Table III. A comparison with Table II shows that the magnetic structure above 4.5 °K is in complete accord with the considerations outlined above. However, the situation below 4.5 °K deserves special consideration: The components $C_z(Er^{3+})$ and $G_y(Fe^{3+})$ belong to $Pbnm$, $G_x(Fe^{3+})$ to $Pb'n'm$, and $F_x(Fe^{3+})$ to $Pbn'm'$. The coexistence of these components thus implies a decrease from orthorhombic to monoclinic symmetry (Table III). Furthermore, it is difficult to see how an antiferromagnetic component G_x and a ferromagnetic component F_x will coexist along the common *a* crystallographic axis. In view of these difficulties, we have decided to reexamine the magnetic structure of $ErFeO_3$ below 4.5 °K.

II. MAGNETIC STRUCTURE AT 1.5 °K—NEUTRON DIFFRACTION

Neutron ($\lambda \sim 2.4$ Å) diffraction patterns of a polycrystalline sample of $ErFeO_3$ were taken at 140, 4.2, and 1.5 °K. The resulting patterns are shown in Fig. 2. The relatively long neutron wavelength was used in order to obtain good angular resolution. Oriented (±3.5°) graphite, 50 mm thick, was placed in the beam between the monochromator and the sample in order to eliminate any high-order contamination in the beam.[10] The observed integrated intensities of these pattern are listed in Table IV.

TABLE II. Possible magnetic structures in the (4*b*) and (4*c*) positions in D_{2h}^{16} with symmetry isomorphic (Ref. 5) with D_{2h}^{16}. (G_α with $\alpha = x, y, z$ designates a *G* configuration with the spin axis along *a*, *b*, *c*, respectively, etc.)

Space group	(4*b*)	(4*c*)
$Pbnm$	$A_x\ G_y\ C_z$	⋯ ⋯ C_z
$Pbn'm'$	$F_x\ C_y\ G_z$	$F_x\ C_y$ ⋯
$Pb'nm'$	$C_x\ F_y\ A_z$	$C_x\ F_y$ ⋯
$Pb'n'm'$	$G_x\ A_y\ F_z$	⋯ ⋯ F_z
$Pb'n'm'$	⋯ ⋯ ⋯	$G_x\ A_y$ ⋯
$Pb'nm$	⋯ ⋯ ⋯	⋯ ⋯ A_z
$Pbn'm$	⋯ ⋯ ⋯	⋯ ⋯ G_z
$Pbnm'$	⋯ ⋯ ⋯	$A_x\ G_y$ ⋯

TABLE III. Published magnetic structures of $ErFeO_3$.

Temperature range (°K)	Fe (4*b*) sublattice	Er (4*c*) sublattice	Space group	Ref.
620 − 100	G_x ⋯ F_z	⋯ ⋯ ⋯	$Pb'n'm$	6–10
90 − 4.5	F_x ⋯ G_z	⋯ ⋯ ⋯	$Pbn'm'$	6–10
4.5 − 1.25	$G_xF_x\ G_y$ ⋯	⋯ ⋯ C_z	$P2_1/m$	6–9

In determining the magnetic structure at 1.5 °K it was assumed that (i) the magnetic structure of the Er lattice is C_z, as was found by Koehler *et al.*[9] This identification is evident from the appearance of the {010} and {100} diffraction peaks in Fig. 2. (ii) The magnetic configuration of the Fe lattice is essentially *G*, as was reported by Koehler *et al.*[9] This identification is evident from the appearance of the {011} and {101} diffraction peaks in Fig. 2. (iii) The antiferromagnetic spin axis of the Fe lattice is perpendicular to at least one of the crystal axes *a*, *b* or *c*. The symmetry of this class of structures is higher than that corresponding to structures with an arbitrary direction of the antiferromagnetic spin axis. The spin reorientation at ~100 °K in $ErFeO_3$ satisfies this restriction,[11] and as we shall show, spin structures satisfying this restriction do exist in our case; hence, structures having a lower symmetry were not considered.

With these assumptions, the structure determination reduces to a search for that direction of the antiferromagnetic axis of the Fe^{3+} spin system with-

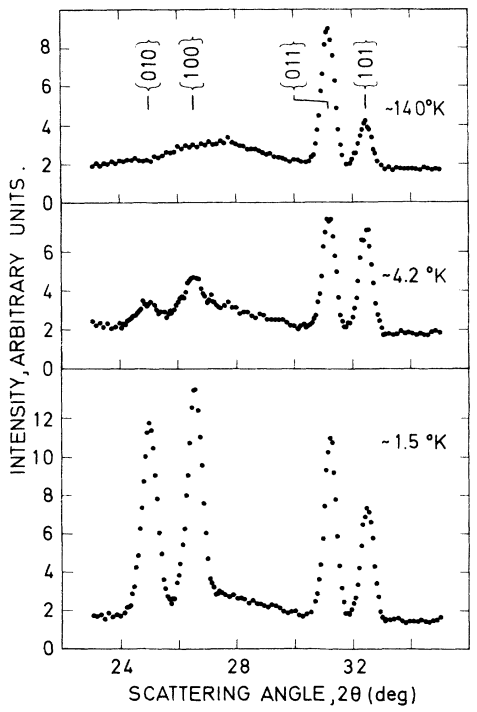

FIG. 2. Neutron ($\lambda \sim 2.4$ Å) diffraction patterns of $ErFeO_3$ at 140, 4.2, and 1.5 °K.

TABLE IV. Observed integrated intensities.

	I_{obs}		
$\{hkl\}$	140 °K	4.2 °K	1.5 °K
{010}	•••	2 770 ± 400	18 850 ± 410
{100}	•••	3 270 ± 400	20 174 ± 375
{011}	11 427 ± 173	10 058 ± 168	14 827 ± 175
{101}	3 714 ± 144	9 068 ± 160	9 343 ± 155

in the crystallographic planes *ab*, *ac*, and *bc* which will best fit the observed integrated intensities. In determining the quality of a given fit, we used the following three criteria.

a. *The discrepancy factor R.* We defined a discrepancy factor

$$R = 100 \sum \left| \frac{I_{obs}}{\sum I_{obs}} - \frac{I_{calc}}{\sum I_{calc}} \right| , \tag{1}$$

where the summations were carried out over the integrated intensities[12] of the four lines listed in Table IV at 1.5 °K. Since these four lines do not contain (practically) any nuclear contribution, it was possible to calculate R as a function of two parameters: μ_{Er}/μ_{Fe} and the angle $\vec{\mu}_{Fe}$ makes with one of the crystal axes. Here μ_M is the ionic magnetic moment on an M (M = Er, Fe) site. R was subsequently calculated for μ_{Fe} in the *ab*, *ac*, and *bc* planes for $1.2 < \mu_{Er}/\mu_{Fe} < 1.8$. The results of these calculations for the positive quadrants of the *ab*, *ac*, and *bc* planes are shown in Fig. 3. We see that there are rather well-defined regions of low (< 2%) R within each of the three quadrants. These low-R regions were next examined against the other criteria.

b. *The temperature dependence of the intensity of the* {101} *line.* The {101} line is essentially magnetic in origin, with the magnetic contribution coming only from the Fe^{3+} spin system. At 1.5 °K the Fe^{3+} spin configuration is of the G type. Let α, β, γ be the direction cosines of the Fe^{3+} spin axis with respect to the a, b, and c axes, respectively. It then follows[12] that

$$I_G^{101} \simeq 1 - \frac{\alpha^2/a^2 + \gamma^2/c^2}{1/a^2 + 1/c^2} , \tag{2}$$

where I_G^{101} is the calculated integrated intensity of {101} (for a G-type configuration) and a, c are unit-cell dimensions. Now, it is well known[7] (Table III) that at 140 °K the structure is G_x. Hence, at 140 °K we have

$$I_{G_x}^{101} \simeq \frac{a^2}{a^2 + c^2} . \tag{3}$$

The experimental ratio (see Table IV)

$$\frac{I_{obs}^{101}(1.5\ °K)}{1.018\, I_{obs}^{101}(140\ °K)} = 2.47 \pm 0.13 \tag{4}$$

is now set equal to $I_G^{101}/I_{G_x}^{101}$. The coefficient in the denominator is introduced in order to account for the nonsaturation of I_{obs}^{101} at 140 °K. For $c^2/a^2 = 2.08$[13] we then obtain

$$2.08\alpha^2 + \gamma^2 = 0.61 \pm 0.13 . \tag{5}$$

The direction cosines must also satisfy

$$\alpha^2 + \beta^2 + \gamma^2 = 1. \tag{6}$$

We considered, in accordance with our earlier assumptions, only those solutions of Eqs. (5) and (6) in which the spin axis was perpendicular to one of the crystal axes. (i) For $\gamma = 0$, $\beta = \pm (0.84 \pm 0.04)$. Here the spin axis is in the *ab* plane making an angle of $\pm (33° \pm 4°)$ with the b direction. (ii) For $\alpha = 0$, $\beta = \pm (0.62 \pm 0.11)$. Here the spin axis is in the *bc* plane making an angle of $\pm (51° \pm 8°)$ with the b direction. (iii) For $\beta = 0$, no solution. Thus the spin axis can not be in the *ac* plane. Our second criterion has therefore eliminated any possible solution in the *ac* plane. The regions allowed by the solutions (i) and (ii) are marked in Fig. 3 by pairs of dashed lines centered about the angles 33° (in the *a b* plane) and 51° (in the *bc* plane).

c. *The ratio* μ_{Er}/μ_{Fe}. We have calculated the ratio μ_{Er}/μ_{Fe} from the lines {011}, {101} (140 °K) and {010}, {100} (1.5 °K). These lines are due to magnetic contributions from the Fe^{3+} and Er^{3+} spin

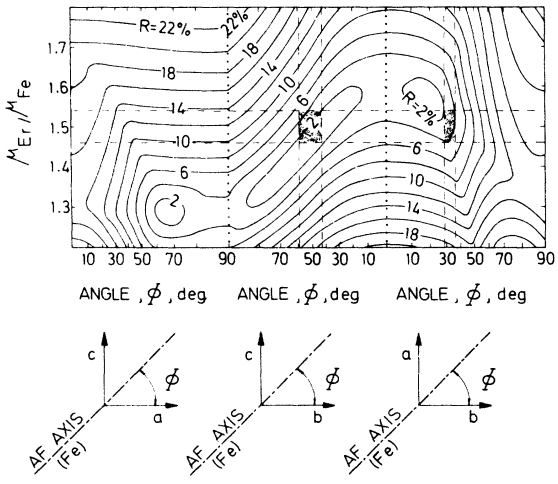

FIG. 3. Discrepancy factor, R, contours for various μ_{Er}/μ_{Fe} in the positive quadrants of the *ab*, *ac*, and *bc* planes. The vertical and horizontal dashed lines mark the bounds for structures satisfying criteria 2 and 3, respectively. The shaded areas mark the regions simultaneously satisfying both criteria 2 and 3.

TABLE V. Calculation of $\langle C\mu_M^2 \rangle$.

$\{hkl\}$	Sublatt. M	Magnet struct.	I'_{calc}	$C\mu_M^2$ [a]	$\langle C\mu^2 \rangle$
{010}	Er	C_z	131.6	143.2 ± 3.1	144 ± 3
{100}			139.6	144.5 ± 2.7	
{011}	Fe	G_x	188.61	60.6 ± 0.9	64 ± 2[c]
{101}			55.71	65.3 ± 2.5[b]	

[a]With $C\mu_M^2 = I_{obs}(T)/I'_{calc}$ with $T = 1.5$ and 140 °K for the Er and the Fe sublattice, respectively.

[b]After subtraction of a nuclear contribution of 2% to I_{obs} (140 °K).

[c]After adding a 1.8% correction to account for the non-saturation of I_{obs} (140 °K).

systems, respectively. Let us define the intensity per unit magnetic moment

$$I'_{calc} = I_{calc}/\mu_M^2 \ ,$$

where

$$M = \begin{cases} \text{Fe for } \{011\},\ \{101\} \\ \text{Er for } \{010\},\ \{100\} \end{cases} , \tag{7}$$

where I_{calc} is the calculated integrated intensity.[12] We then have

$$I_{obs} = C\mu_M^2 I'_{calc} \ , \tag{8}$$

where C is an experimental factor fixed for all lines. The numerical values of I_{obs}/I'_{calc} are given in Table V. When averaged over the respective pairs, they yield $\langle C\mu_{Er}^2 \rangle = 144 \pm 3$ and $\langle C\mu_{Fe}^2 \rangle = 64 \pm 2$, hence

$$\mu_{Er}/\mu_{Fe} = (144 \pm 3/64 \pm 2)^{1/2} = 1.50 \pm 0.04 \ . \tag{9}$$

The region allowed by this solution is marked in Fig. 3 by the pair of dashed lines centered about $\mu_{Er}/\mu_{Fe} = 1.5$.

In Fig. 3, in which R is mapped for the spin axis in the positive quadrants of the ab, bc, and ac planes, we have marked (shaded area) the two regions simultaneously satisfying criteria 2 and 3. One region is in the bc plane with $\sphericalangle(\vec{\mu}, \vec{b}) = 51° \pm 8°$ and the other is in the ab plane with $\sphericalangle(\vec{\mu}, \vec{b}) = 33° \pm 4°$. As for criterion 1 (low R), both of the shaded regions in Fig. 3 seem to be acceptable with the former being somewhat more favorable (lower R). Although not shown, R values were also calculated for the other six quadrants[14] which contain b, i.e., $\bar{a}b$, $a\bar{b}$, $\bar{a}\bar{b}$, $\bar{b}c$, $b\bar{c}$, and $\bar{b}\bar{c}$. These calculations showed that none of the low-R regions in these quadrants satisfy criteria 2 and 3. As for the quadrants in the ac plane, an R calculation was not necessary as criterion 2 is not satisfied in the entire ac plane (no solution for $\beta = 0$). Thus we conclude that there are only two structures (with $\vec{\mu}_{Fe}$ perpendicular to at least one of the crystal axes) that give a satisfactory fit to the diffraction data. The first, with the spin axis in the ab plane and $\phi_1 = \sphericalangle(\vec{\mu}, \vec{b}) \simeq 33°$, is shown in Fig. 4(a). This is essentially the structure proposed by Koehler *et al.*[9] The second somewhat more favorable structure (lower R), with the spins in the bc plane and $\phi_2 = \sphericalangle(\vec{\mu}, \vec{b}) \simeq 51°$, is shown in Fig. 4(b).

III. WEAK FERROMAGNETISM

In order to further clarify the nature of the low-temperature spin structure, magnetization data at temperatures down to 1.9 °K and in applied magnetic fields up to 50 kG were recorded using a vibrating-sample magnetometer. In Fig. 5 we show the measured temperature dependence of the spontane-

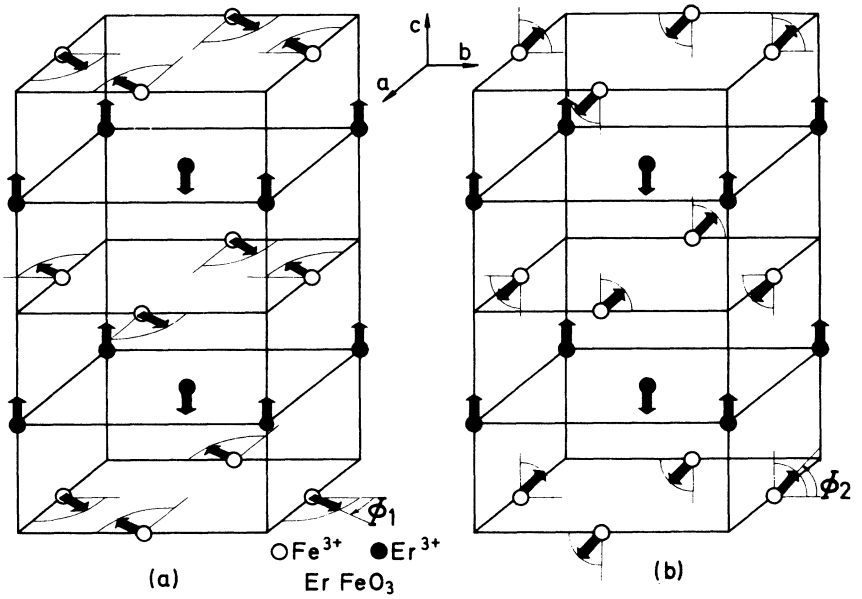

FIG. 4. Two possible magnetic structures consistent with the 1.5 °K neutron diffraction data. (a) Structure 1 is similar to that found by Koehler *et al.* (b) Structure 2, on the other hand, is somewhat more favorable (lower R) according to the present analysis.

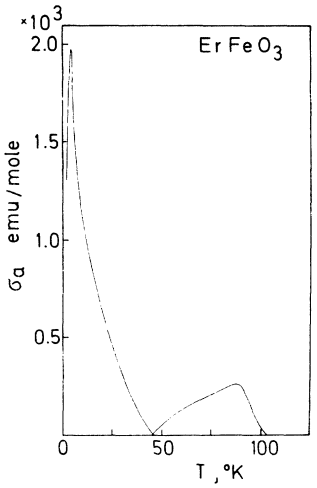

FIG. 5. Temperature dependence of the spontaneous magnetic moment of $ErFeO_3$ in the *a* direction.

ous magnetization in the [100] direction.[15] In order to avoid a multidomain state in the crystal, a low magnetic field (50 G) was applied along the ferromagnetic axis while the measurements shown in Fig. 5 were carried out.

The observed temperature dependence is attributed[7,16] to a negative coupling coefficient between the spins of the rare-earth ions and the Fe^{3+} canted-spin structure; i.e., the net polarizations of the Er^{3+} spin system is antiparallel to the weak ferromagnetic moment of the Fe^{3+} spins. Below the first spin reorientation region (i.e., 100–90 °K), the contribution of the Er^{3+} spins to the total magnetic moment increases at a higher rate than that of the Fe^{3+} spins as the temperature is decreased. As a result of this a compensation point occurs at $T \simeq 45$ °K where the contributions of the two spin systems to the total moment are equal and opposite. Upon further cooling, the direction of the magnetic moment reverses and its magnitude increases monotonically until a temperature of $T \simeq 4.5$ °K is reached. At this point, the temperature dependence of the magnetic moment changes sign and decreases quite sharply as the temperature is further decreased to 1.9 °K. However, torque measurements carried out in the 1.9 to 4.5 °K temperature region do not show any angular deviation of the spontaneous magnetization away from the *a* crystallographic axis. Thus we conclude that the antiferromagnetic axis of the Fe^{3+} spin system is confined to the *bc* plane since, as is clear from Table II, there would otherwise appear a ferromagnetic moment along the *c* axis.

The field dependence of the magnetization at 4.2 and 2 °K, as measured along the orthorhombic axes, is shown in Fig. 6. By extrapolating the 4.2 °K set of curves to $H=0$, one observes that the spontaneous magnetic moment lies along the *a* axis. At 2 °K, a metamagneticlike transition is observed in the *c* direction. This effect indicates an ordering of the Er^{3+} spin system along the *c* axis, in agreement with the neutron diffraction results of Sec. II. Note further that at 2 °K no spontaneous moment is observed along the *c* axis, thereby supporting our conclusion that the weak ferromagnetic moment of $ErFeO_3$ remains along the *a* crystallographic axis for $1.9 < T < 4.5$ °K.

IV. DISCUSSION

We have found, in Sec. II, that there are two possible structures for the Fe^{3+} spin system at 1.5 °K that are in satisfactory agreement with the neutron diffraction data. In the first [structure 1, Fig. 4(a)], the spins lie in the *ab* plane with the antiferromagnetic axis at an angle of 33° to the crystallographic *b* axis. This is the structure first suggested by Koehler *et al.*[9] and, more recently, by Pataud and Sivardiere,[17] on the basis of their respective neutron diffraction studies. However, we have seen that this structure assignment is not an unambiguous one. The alternate structure [structure 2, Fig. 4(b)], in which the spins lie in the *bc* plane at an angle of 51° to the *b* axis, is also an acceptable interpretation of the diffraction data.

To distinguish between the two possible structures, we must turn to the magnetization data presented in Sec. III. In structure 1, the Fe^{3+} spins are essentially in a mixed G_{xy} mode. Owing to the antisymmetric exchange interaction[16] between the Fe^{3+} spins, there must be a weak ferromagnetic moment in the *c* crystallographic direction (F_z) associated with such a structure. On the other hand, in structure 2, the Fe^{3+} spins are essentially in a

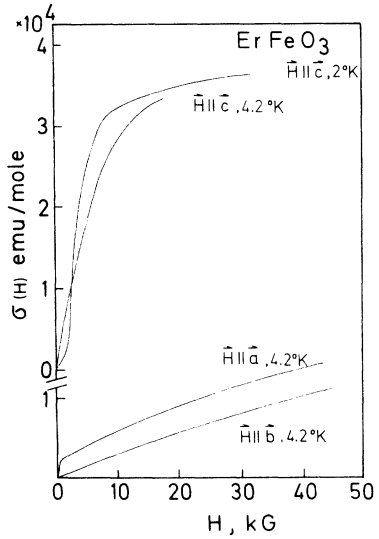

FIG. 6. Field dependence of the magnetization of $ErFeO_3$ for fields applied along the crystallographic axes at 4.2 and 2 °K.

mixed G_{yz} mode and the antisymmetric exchange will result in a weak ferromagnetic moment parallel to the a crystallographic axis (F_x). Since the spontaneous magnetization is in fact along the a axis in the 1.9 to 4.5 °K temperature range, it follows that the low-temperature phase of $ErFeO_3$ is described by the mixed spin mode $G_{yz}F_x$ (structure 2). Thus we conclude that, as the temperature is lowered below 4.5 °K, the Fe^{3+} antiferromagnetic spin axis turns gradually from the c toward the b crystallographic axis and, at 1.5 °K, makes an angle of approximately 51° with the latter axis.

This rotation of the Fe^{3+} spins is a consequence of the exchange coupling between the Fe^{3+} and Er^{3+} magnetic moments. Both Mössbauer[18] and optical spectroscopy[19] studies have shown that the ground-state splitting of the Er^{3+} ion increases sharply as the temperature is reduced below 4.5 °K. Further, the Er^{3+} spin system is known, from all the neutron diffraction studies, to be in essentially a C_z mode in this temperature range. In other words, the Er^{3+} spin changes from a C_zF_x to an essentially C_z mode in a relatively narrow temperature region in the neighborhood of 4.5 °K. This should result in an observable anomaly in the specific heat and such a peak has been reported at approximately 4 °K by Pataud and Sivardiere.[20]

Finally, we note that the mechanism underlying this low-temperature spin reorientation is still not completely clear. One possible mechanism is an Er-Er interaction leading to a cooperative ordering of the Er^{3+} spin in a C_z mode at $T_N(Er^{3+}) \simeq 4.5$ °K. This mode could then couple to the G_y mode of the Fe^{3+} moments,[4] leading to a gradual $G_z \rightarrow G_y$ rotation of the Fe^{3+} spin system as the temperature is further lowered below $T_N(Er^{3+})$ and the magnitude of the Er^{3+} moments increases. Faulhaber *et al.*[19] and others[18,21] have suggested that this is indeed the case, with the Er-Er interaction beginning because of the dipolar field of the Er^{3+} moments. The dipole-dipole interaction does not however appear to be strong enough to induce such a cooperative ordering in $ErFeO_3$ at 4.5 °K. The isomorphic compound $ErAlO_3$ is known to order cooperatively in a C_z mode only at 0.6 °K.[22] Thus, unless the Er^{3+} magnetic moment in $ErAlO_3$ is much less than that in $ErFeO_3$, it is unlikely that a cooperative ordering of the Er^{3+} spin system underlies the low-temperature spin reorientation.

An alternate possibility is that the reorientation is induced primarily by the Fe-Er exchange interaction. Wood *et al.*[23] have shown that the g factors of the low-lying Kramer's doublet of $ErFeO_3$, in their local principal axis system, are $g_\xi = 1.2$, $g_\eta = 4.5$, and $g_\zeta = 5.76$. Here ξ and η lie in the $a\,b$ plane and ζ is along the c axis. For temperatures somewhat above 5 °K, the Fe^{3+} exchange field is in the $a\,b$ plane and the Er^{3+} moments are essentially along the local η axis.[21] If, however, this same exchange field were to lie along the c axis rather than in the $a\,b$ plane it is clear that that part of the system free energy due to the Fe-Er interaction would be lowered, since $g_z > g_y$. Now a c-direction effective field will exist if the Fe^{3+} spin system, in whole or in part, is in a G_y configuration. Thus we see that the Fe-Er interaction can also, in principle, lead to a rotation of the Fe^{3+} spin axis. Pataud and Sivardiere[20] and also Belakhovsky *et al.*[24] have suggested that this is the mechanism responsible for the spin reorientation.

In summary, we had found from neutron diffraction and magnetization studies that the low-temperature ($T < 4.5$ °K) magnetic structure of the Fe^{3+} spin system in $ErFeO_3$ is $G_{yz}F_x$. The antiferromagnetic axis of the Fe^{3+} spin system rotates from the c toward the b crystallographic axis as T is lowered below 4.5 °K, making an angle of $51° \pm 8°$ to b at 1.5 °K. Either an Er-Er or the Fe-Er interaction (or a combination of both) could be the mechanism responsible for the spin reorientation. Further studies will be required to make a final determination.

ACKNOWLEDGMENT

We are grateful to Professor S. Shtrikman for many helpful discussions and suggestions throughout the course of this work.

*Supported in part by the Air Force Materials Laboratory (AFSC) through the European Office of Aerospace Research under Grant No. AFOSR 72-2327.

[1]S. Geller and E. A. Wood, Acta Crystallogr. **9**, 563 (1956).
[2]These configurations transform as irreducible representations of the paramagnetic space group $1'$ *Pbnm* with $\vec{k} = 0$.
[3]E. O. Wollan and W. C. Koehler, Phys. Rev. **100**, 545 (1955).
[4]E. F. Bertaut, in *Magnetism*, edited by G. T. Rado and H. Suhl (Academic, New York, 1963), Vol. III.
[5]These structures transform as irreducible representations of the paramagnetic space group $1'$ *Pbnm* with $\vec{k} = 0$.
[6]R. M. Bozorth, V. Kramer, and J. P. Remeika, Phys. Rev. Lett. **1**, 3 (1958).
[7]R. L. White, J. Appl. Phys. **40**, 1061 (1969).
[8]J. B. Goodenough and J. M. Longo, in *Landolt-Bornstein III/4a, 126* (Springer-Verlag, Berlin, 1970).
[9]W. C. Koehler, E. O. Wollan, and M. K. Wilkinson, Phys. Rev. **118**, 58 (1960).
[10]The spin reorientation region of $ErFeO_3$ has been studied by several authors. See, for example, H. Pinto, G. Shachar, H. Shaked, and S. Shtrikman, Phys. Rev. B 3, 3861 (1971).
[11]H. Pinto and H. Shaked, Nucl. Instrum. Methods **97**, 71 (1971).
[12]Z. Fridman, H. Pinto, H. Shaked, G. Gorodetsky, and S. Shtrikman, Int. J. Magn. **2**, 409 (1971). A general expression for the calculated integrated intensity is given in G. E. Bacon, *Neutron Diffraction* (Oxford U. P., London, 1962), pp. 96 and 163.
[13]M. Eibschütz, Acta Crystallogr. **19**, 337 (1965).
[14]For example, in the calculations for the $\bar{a}\,\bar{b}$ quadrant, the

magnetic moment of Fe^{3+} ion No. 1 (Fig. 1) lies in the $\bar{a}\,\bar{b}$ quadrant. Since the magnetic structure of the Er^{3+} system is always C_z with Er^{3+} ion No. 1 (Table I, Fig. 1) taken to be in the positive c direction, R values calculated for $\bar{a}\,\bar{b}$ are, in general, different than those calculated for $a\,b$.

[15]The spontaneous magnetic moment has also been measured by A. Malozemoff (see Ref. 7). His results exhibit a slightly wider reorientation region and a somewhat smaller moment at 4.2 °K than those presented here.

[16]G. Gorodetsky and D. Treves, *Proceedings of the International Conference on Magnetism, Nottingham, 1964* (The Insitute of Physics and The Physical Society, London, 1964), p. 606.

[17]P. Pataud and J. Sivardiere, J. Phys. (Paris) **31**, 803 (1970).

[18]W. Wiedmann and W. Zinn, Z. Angew. Phys. **20**, 327 (1966).

[19]R. Faulhaber, S. Hüfner, E. Orlich, and H. Schuchert, Z. Phys. **204**, 101 (1967).

[20]P. Pataud and J. Sivardiere, J. Phys. (Paris) **31**, 1017 (1970). The author's interpretation of their results in terms of a G_z-G_{xy} reorientation of the Fe^{3+} spin system (see Ref. 17) is not in accordance with the results of our study as presented here.

[21]I. Nowik and H. H. Wickman, Phys. Rev. Lett. **17**, 949 (1966).

[22]J. Sivardiere and S. Quezel-Ambrunaz, C.R. Acad. Sci. B **273**, 619 (1971).

[23]D. L. Wood, L. M. Holmes, and J. P. Remeika, Phys. Rev. **185**, 689 (1969).

[24]M. Belakhovsky, J. Chappert, J. Ruoskov, and J. Sivardiere, J. Phys. (Paris) **32**, C1–492 (1971). Here again, the authors interpretation of their results in terms of a G_z-G_{xy} reorientation of the Fe^{3+} spin system is not in accordance with the results of our study.